

# PROCEEDINGS OF SPIE

[SPIDigitalLibrary.org/conference-proceedings-of-spie](https://SPIDigitalLibrary.org/conference-proceedings-of-spie)

## Modeling countermeasures to imaging infrared seekers

Laurence Cox, Michael Batten, Stephen Carpenter, Philip Saddleton

Laurence J. Cox, Michael A. Batten, Stephen R. Carpenter, Philip A. B. Saddleton, "Modeling countermeasures to imaging infrared seekers," Proc. SPIE 5615, Technologies for Optical Countermeasures, (29 December 2004); doi: 10.1117/12.580550

**SPIE.**

Event: European Symposium on Optics and Photonics for Defence and Security, 2004, London, United Kingdom

# Modelling countermeasures to imaging infrared seekers

L. J. Cox<sup>a</sup>, M. A. Batten<sup>b</sup>, S. R. Carpenter<sup>a</sup>, P. A. B. Saddleton<sup>b</sup>

<sup>a</sup> Sensors Department, Dstl, Farnborough, Hampshire, GU14 0LX, UK

<sup>b</sup> EDS Defence Ltd, Hook, Hampshire, RG27 9XA, UK

## ABSTRACT

The threat to aircraft from missiles with imaging infrared seekers has developed more rapidly and in more countries independently than the original infrared missile threat<sup>1</sup>. This is, in part, a consequence of the civil sector's demand for high-resolution infrared imagers and the development of computer processors capable of implementing complex image-processing algorithms in real time. Dstl has developed the Fly-In model to analyse the potential effectiveness of existing countermeasures (CM) to imaging infrared seekers and to test new CM approaches before trialling them against surrogate imaging seekers<sup>2</sup>.

The validation of the Fly-In model is extremely important, particularly as the newness of the imaging infrared threat, means that actual examples of the threat are not available for study. Extensive measurements have been carried out on the appearance of flare CM in different infrared wavebands, and on the effects of lasers on the optics and detector of an surrogate imaging seeker. Other parts of the model are derived from other Dstl models, including the NATO Infrared Airborne Target Model (NIRATAM) and HADES (missile dynamics) that are validated against trials' data.

Initial studies have shown that existing CM, and those under development, can be very effective against imaging infrared seekers, by defeating the seeker's image-processing algorithms. It is already clear that laser CM will play an increasing role in the defence of aircraft, thereby enhancing aircraft survivability. Moreover, this model will aid the military planner in determining the best mix of CM and the tactics for using them.

## 1. THE FLY-IN MODEL

Dstl currently investigates the potential effectiveness of Infrared Countermeasures (IRCM), including laser-based IRCM, in decoying anti-air missiles with imaging infrared seekers. EDS Defence Ltd (EDL) have supported this research programme for a number of years by developing with Dstl the Fly-In engagement model, which simulates the engagement of an aircraft with countermeasures (CM) by a missile with a imaging infrared seeker.

Research into IRCM to imaging seekers began at Dstl in 1986, with the development of tools for mathematical modelling of the image processing function. The development of the Fly-In model started in 1990. In 1997, a decision was made to transfer it to a Windows NT-based platform, and recode the model in C++ using modular object-oriented principles. Since then, the model (now called Fly-In 2000) has been developed further on this platform. The modules represent:

- background;
- aircraft;
- clouds;
- sun;
- countermeasures;
- atmosphere; scene generator;
- sensor;
- image processing;
- missile dynamics.

The heart of the model (Figure 1) is the scene generator module that takes data from the background, aircraft, cloud, Sun, countermeasure and atmosphere modules to form a radiance map of the scene at the location of the sensor. A wide

range of backgrounds can be simulated including sky, urban and rural land, and sea backgrounds using fractal-based models of data gathered using IR cameras on trials' aircraft. The aircraft module uses the same faceted data files as the airframe models used in NIRATAM, but users can also create their own aircraft models from commercially-available wire-frame models by adding temperature and emissivity information for each facet. Countermeasures models are based on measurements gathered at trials, but examples of similar countermeasures can be found in Volume 7 of The Infrared and Electro-Optical Systems Handbook<sup>3</sup>.

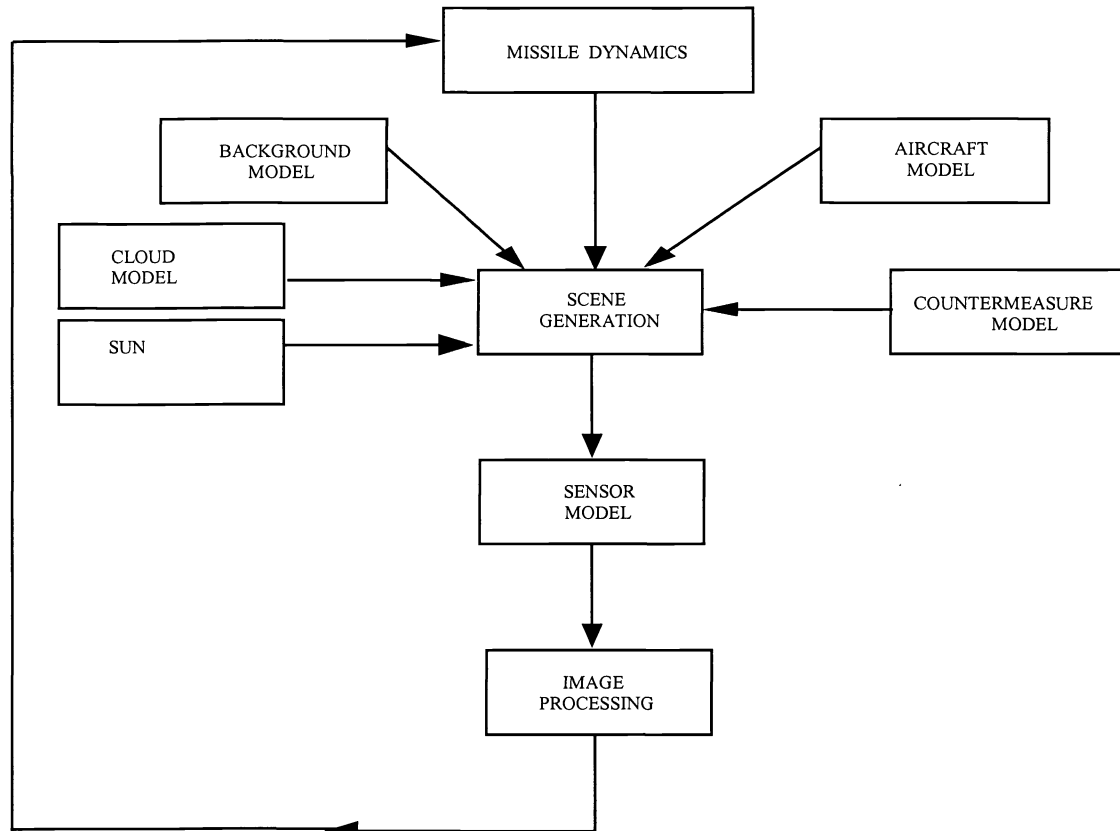


Figure 1. Fly-In architecture

The sensor module converts the output of the scene generator into an image radiance map by applying the optics' Point Spread Function (PSF). The image is sampled at a spatial frequency corresponding to the detector pitch, the photon flux converted to the number of electrons in each well and noise terms are added. The sampled image is then quantised and saturation effects included.

The image-processing module operates on the set of grey levels that represent the image. This performs object extraction, target tracking and CM rejection functions; currently it uses one of two target tracking algorithms called ATAGS and PentA. ATAGS (Automatic Target Acquisition and Guidance System) uses edge and feature extraction to identify targets for tracking. PentA (Advanced Anti-Air Acquisition Algorithm) uses neural network algorithms to extract targets from the scene. ATAGS represents a level of algorithmic complexity that could be implemented using information from the open literature<sup>4</sup>, whilst PentA represents the state-of-the-art that might be found in modern imaging seekers although it is a completely separate line of development. The flexibility of the model is such that image processing algorithm modules can be developed by other nations and included in the model.

Target-tracking data are used to steer the missile, whose motion is controlled by the dynamics module. This contains a six degrees-of-freedom (6 DoF) representation of the missile that performs a proportional navigation (PN) flight path with a damped "g" response and a velocity profile based on the missile thrust and drag. This representation is derived

from Dstl's HADES model. The missile dynamics module moves the missile to its position at the end of the next timestep so that, when combined with aircraft and countermeasure movements, the scene generator module can generate the radiance image for the next frame.

Although the description above is for a one-on-one engagement, and this is how Fly-In is normally used, the number of aircraft, countermeasures and missiles in a simulation is not limited. The only effect of increasing the number of entities (the generic term used to describe aircraft, countermeasures and missiles) in the scene is to slow the simulation frame rate. As the missile is simulated entirely in software, there is no requirement for the simulation to operate in real time.

To illustrate the fidelity of the scene generation, sensor, and image processing modules, Figure 2 shows a radiance map (top left) of a target releasing a CM, with the resulting sensor image (top right) after being blurred by the PSF, quantisation and the addition of noise. The figure also shows the results of edge extraction (bottom left) and object extraction (bottom right) in the ATAGS image-processing module. The small crosses visible in the sensor and image processing images in Figure 2 are the aim-points for the current and last frames.

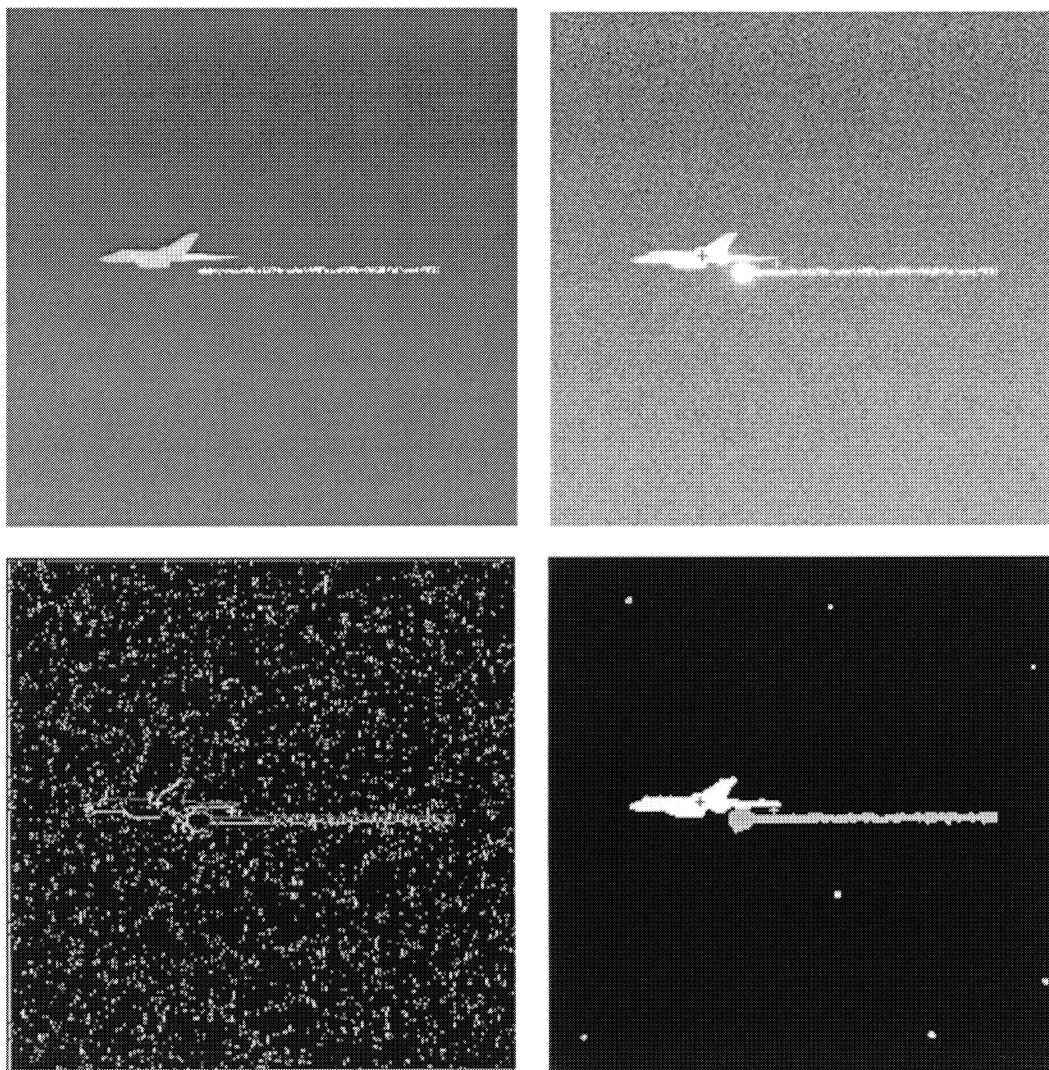


Figure 2. Stages in the processing of the image of a fast jet releasing a flare

Previous versions of Fly-In modelled flares and omni-directional jammer CM only but, with the development of Fly-In 2000, it was modified to represent Directed IRCM (DIRCM)-induced effects also. This required the addition of algorithms to represent the pointing and tracking performance of the DIRCM and the effects of the high-intensity source on the missile sensor. A series of experiments was conducted to build up a database of results as a basis for developing the appropriate algorithms. Some of the experiments and their results are described in the next section.

## 2. EXPERIMENTAL RESULTS

For a typical field-of-view and at typical engagement ranges, an imaging seeker would not spatially resolve a DIRCM, whether a laser or a lamp system, and its geometrical image would be a single pixel on the focal plane. Consequently, two series of experiments were undertaken with point sources, the first using black bodies and the second, lasers. The first series of experiments comprised a high-temperature black body located behind a pinhole. The pinhole was placed several metres in front of a 3-5  $\mu\text{m}$  256 by 256 pixel indium antimonide (InSb) camera so that its angular diameter was exactly one pixel. A shutter was fitted behind the pinhole to blank it off, to give a direct comparison between the image of the source and a bland zero-clutter background. The temperature of the black body was adjusted over a wide range, up to approximately 1,000 K, and the grey level of each pixel in the scene recorded. This allowed each camera pixel to be calibrated and showed that they were linear in their response up to their saturation level. For each temperature, the gradient of the image from pixel to pixel was measured to determine the PSF over a large dynamic range. Using this arrangement, the source corresponded very closely to a DIRCM and a series of experiments were conducted for a variety of lens and camera combinations. A typical image and its simulation in Fly-In are shown in Figure 3.

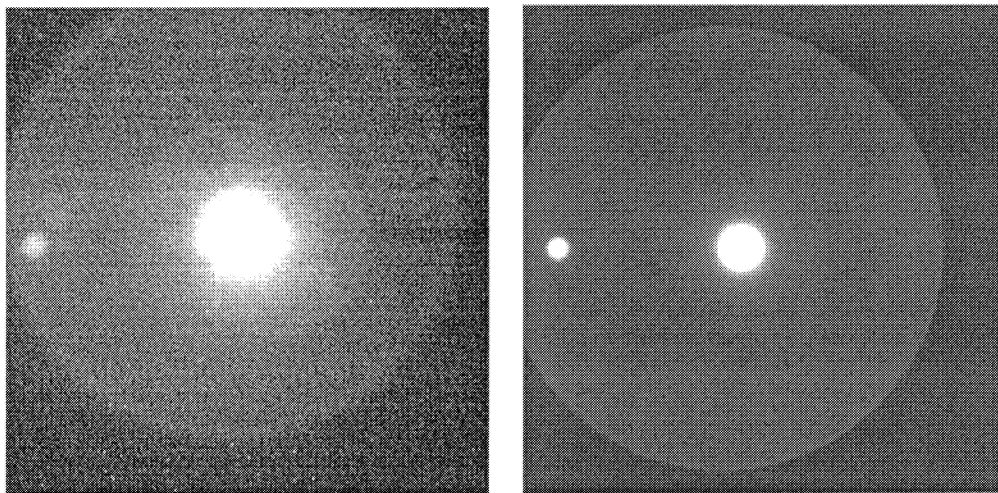


Figure 3. An image of a single-pixel, high-intensity source (left) and its simulation (right)

For all the combinations evaluated the same types of image artefact were observed and categorised as: “geometrical image”, “halo” and “ghost”. The general characteristics of each artefact are described below

- Geometrical image, this was at the anticipated position of the image in the focal plane and had a diameter larger than a single pixel. For practical purposes it was circular and fully saturated with a diameter depending on the incident flux. It represents the minimum image spreading caused by diffraction and optical aberrations.
- Halo, this was considerably larger than the geometrical image and of lower intensity, it was approximately centred on the geometrical image. It was partly caused by scatter in the optics and partly by reflections from optical surfaces close to the detector, such as the dewar window and cold filter.

- Ghost, these could be of any size, in any position and moved at a different angular rate to the geometrical image. A ray-tracing analysis of one lens was undertaken using Code V. This confirmed that the ghosts seen were defocused images caused by multiple reflections from optical surfaces.

The design of any seeker optical system is, necessarily, a compromise between improving optical performance, which tends to lead to more complex designs, and minimising vulnerability to countermeasures. A seeker that has been designed for 'optimum' optical performance may show effects like those above. In particular, once the missile has been flown its IR dome is likely to show some erosion that can considerably increase scatter levels above those measured in the laboratory. Scattering and multiple reflections have both been extensively studied in the past: Chapter 7 of "Applied Optics and Optical Engineering", Volume VII <sup>5</sup> is a very good starting point for the study of scattering from optical surfaces, whilst Cox <sup>6</sup> has analysed multiple reflection and scattering in the 8-12  $\mu\text{m}$  waveband.

The second series of experiments was undertaken using a 3.84  $\mu\text{m}$  continuous wave (CW) deuterium fluoride laser to irradiate several staring-array cameras with cadmium mercury telluride (CMT), InSb and platinum silicide (PtSi) detectors. Figure 4 shows a typical cross section of the signal level (log scale) in a PtSi camera, produced by combining four scans at laser powers covering a wide dynamic range.

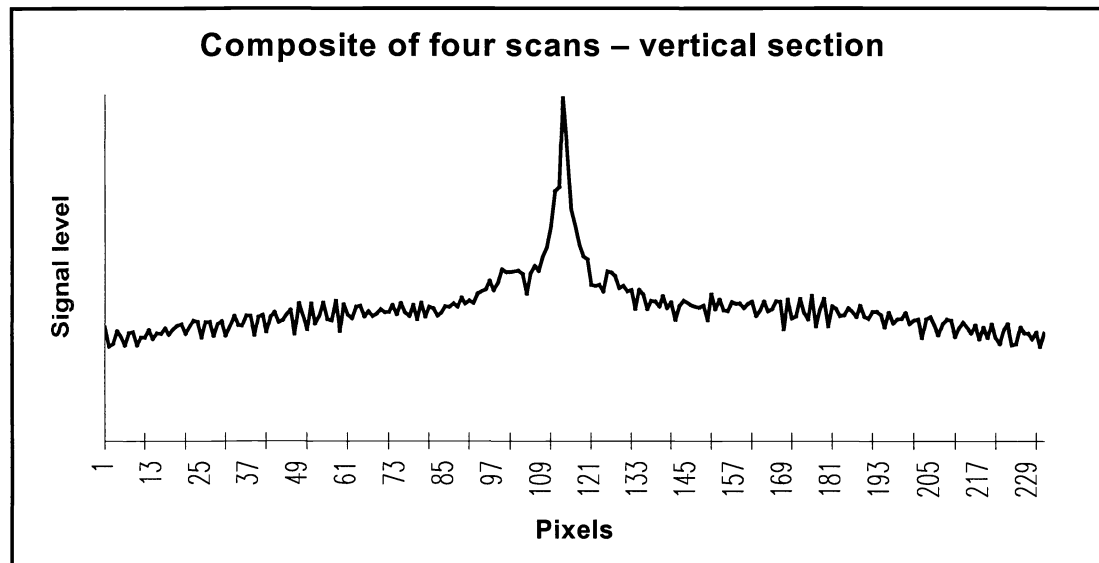


Figure 4. PSF of a PtSi camera

Figure 4 illustrates the same generic characteristics as in the black body experiments described above, that is an intense central maximum surrounded by a plateau or halo.

Figure 5 shows the same results for an InSb array where the signal levels (log scale) at different laser power levels have been superimposed after normalising for laser power. The horizontal lines in this figure are where the detector pixels are saturated; for the lower laser power levels, the graphs have been truncated when the signal approaches the noise level. The good overlap of the curves at widely different power levels shows that the response of the detector is nearly linear, although there is a suggestion of a small degree of non-linearity close to saturation.

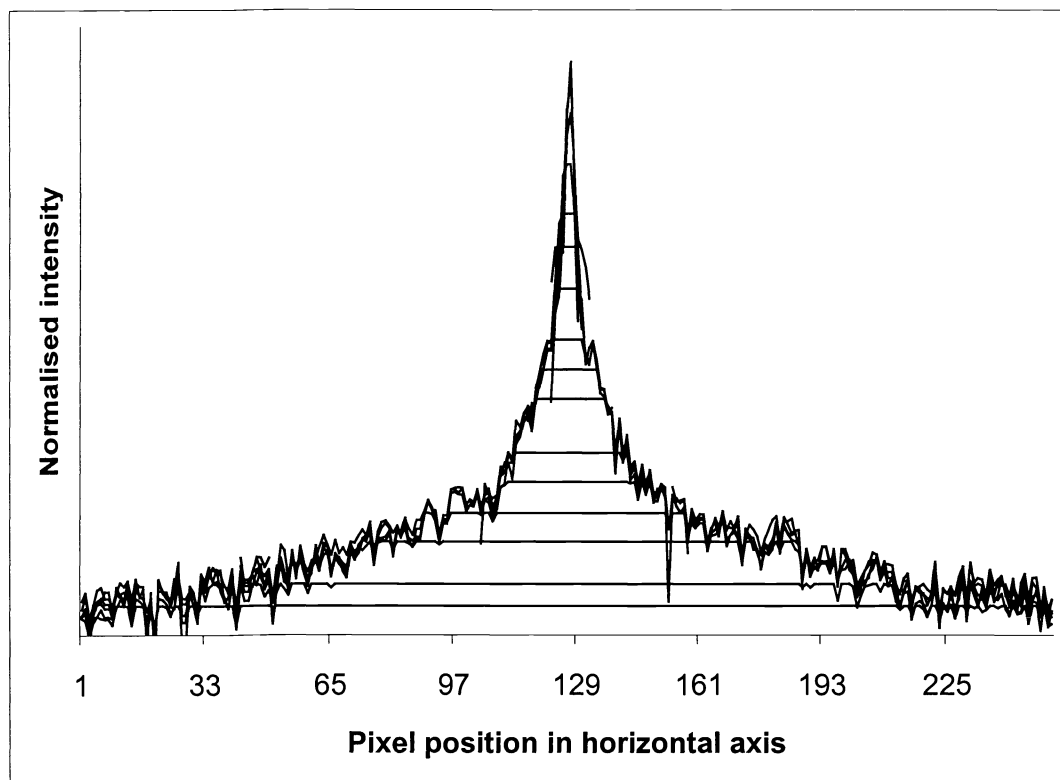


Figure 5. Normalised PSFs for an InSb array at various laser powers

Measurements on InSb and CMT with pulsed lasers have also been made. Although there is not a readily available database, some detector arrays seem to show similar limiting effects to those reported by Kulp et al <sup>7</sup>. Further analysis of these effects is required.

Generic representations of the image artefacts described above have been included in the Fly-In model. This allows it to analyse the complex interactions between target signatures, laser countermeasures, infrared seekers and signal processing algorithms in a non-system-specific manner. The implementation of DIRCM in the Fly-In sensor module is described in the next section.

### 3. DIRCM IMPLEMENTATION IN FLY-IN

A DIRCM system <sup>8</sup>, using either a laser or an arc lamp as the jam source, must be alerted to a threat, and provided with a direction of approach before the system can track it. In Fly-In, a simulated missile warning system alerts the DIRCM system and the beam is pointed at the incoming seeker. The beam-pointing system is in a tracking loop and its irradiance calculated at the seeker. The beam's irradiance at the seeker fluctuates owing to errors in the tracking loop, jitter in the beam director and the effects of atmospheric turbulence. Scintillation is modelled as a log-normal distribution, whose variance is a user-specified function of range. Once the DIRCM irradiance at the seeker has been calculated, it is used to determine the level of the effects described above.

The effects of the DIRCM system are modelled as a modified PSF incorporating the geometric image and halo surrounding it. This is applied isoplanatically, which is across the whole field of view equally. Ghost images are then added but their position varies with the location of the geometric image.

A number of studies have been carried out using DIRCMs modelled in Fly-In. Figure 6 shows some results from one study where a combination DIRCM plus flare CM was used. Providing that the threat is detected at a sufficient range,

this CM proves to be quite effective but if the threat is too close, turning on the DIRCM can cause the threat to effectively ‘home on jam’ and give a lower effectiveness than a flare on its own at the same range. Thus, combinations of CM can show both positive and negative synergy.

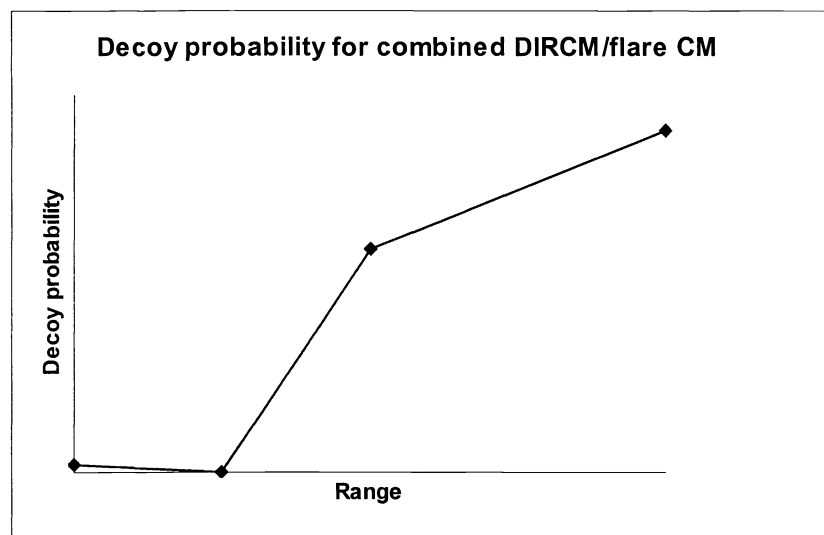


Figure 6. Decoy probability for combined DIRCM/flare CM

Some results from a second study (Figure 7) where only the DIRCM CM was deployed and where it was deployed in conjunction with an aircraft manoeuvre show that the latter can have a significant effect on the miss distance. Although it was not analysed in this study, the Fly-In model also provides data on the tracks of the aircraft and missiles in the simulation that could be input into a aircraft vulnerability model to determine kill probabilities.

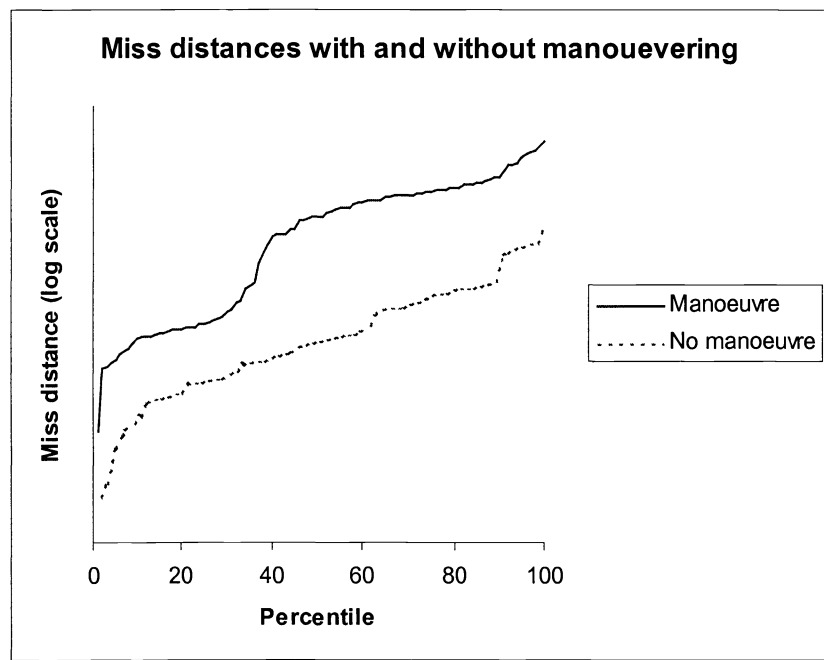


Figure 7. DIRCM-only CM cumulative distribution of miss distances with and without manoeuvre



These studies typically use several thousand runs of the model covering a number of ranges, azimuth and elevation angles, and CM options. On an average PC, each run takes a few minutes to complete, comparable with the time needed for the user to analyse the run. A batch program allows the input data for the set of runs to be prepared in advance, allowing the PC to run continuously. The output data, typically a few megabytes (Mb) per run can be analysed offline.

#### 4. FUTURE DEVELOPMENT

The Fly-In simulation continues to be developed by Dstl and EDL; a new release is planned for March 2005. The current version (v2.3) models single-colour fully-staring arrays, in the next release this is extended to include both multi-colour arrays and scanned linear-arrays. Improvements to target models will include better plume representations and the atmospheric models will be upgraded from LOWTRAN to MODTRAN. The limitations caused by having to run the model on a single processor and manually analyse the output are already evident. The next release will be capable of being run on Dstl's processor farm, and an automated analysis system, based on an enhanced search engine approach, is being developed. This should make possible studies of several hundred thousand runs in the same timescales as the existing studies and increase the use of the model by non-expert professionals in the field.

#### 5. CONCLUSIONS

Fly-In is a mature model framework that allows the countermeasure designer to evaluate potential strategies to defeat the imaging seeker threat. The same issues that have driven the widespread development of the threat: infrared detector arrays, computer processing power and civilian development of image-processing algorithms, also provide the modeller with the tools to counter the threat.

One characteristic of the studies already carried out is that there are often surprising synergistic effects when two or more countermeasures are combined. Moving on from running the model on a single processor and manually analysing the output to running it on a processor farm and automating the analysis, will undoubtedly bring new insights and more effective countermeasure strategies.

Fly-In is distributed to groups collaborating with the UK; for details contact the authors at Dstl Farnborough, UK.

#### 6. ACKNOWLEDGEMENT

The development of this model is supported by UK MoD under the Applied Research Programme, ARP05 RE 508.

#### REFERENCES

1. Hewish M and Lok J J, Arming for close-in air combat, *International Defence Review*, Vol. 32, Iss. 1 (1999)
2. Titterton D H and Carpenter S R, Design and performance of an imaging infra-red-seeker surrogate, *Journal of Defence Science*, Vol. 9, No. 1, ppR7-12 (2004)
3. The Infrared and Electro-Optical Systems Handbook, ERIM/SPIE Press, Vol. 7 – Countermeasures systems, Chapter 3 “Active Infrared Countermeasures” and Chapter 4 “Expendable Decoys” (1993)
4. Sharples G, The development of image processing technologies, *Journal of Defence Science*, Vol. 8, No. 2, pp28-33 (2003)
5. Elson J M, Bennett H E and Bennett J M, “Scattering from Optical Surfaces”, Chapter 7 of *Applied Optics and Optical Engineering*, Volume VII, Eds R R Shannon and J C Wyant, Academic Press 1979
6. Cox L J, Glare in optical systems for thermal band imaging, *Optica Acta*, Vol. 25, No. 12, pp1137-1148 (1978)
7. Kulp T J, Powers P, Kennedy R and Goers U-B, “Development of a pulsed backscatter-absorption gas-imaging system and its application to the visualisation of natural gas leaks” *Applied Optics*, Vol. 37, No. 18, pp3912-3922 (1998).
8. Titterton D H and Payne M J P, The development of airborne laser-based jamming technology, *Journal of Defence Science*, Vol. 3, pp473-480 (1998).

© British Crown copyright 2004/DSTL - published with the permission of the Controller of Her Majesty's Stationery Office.